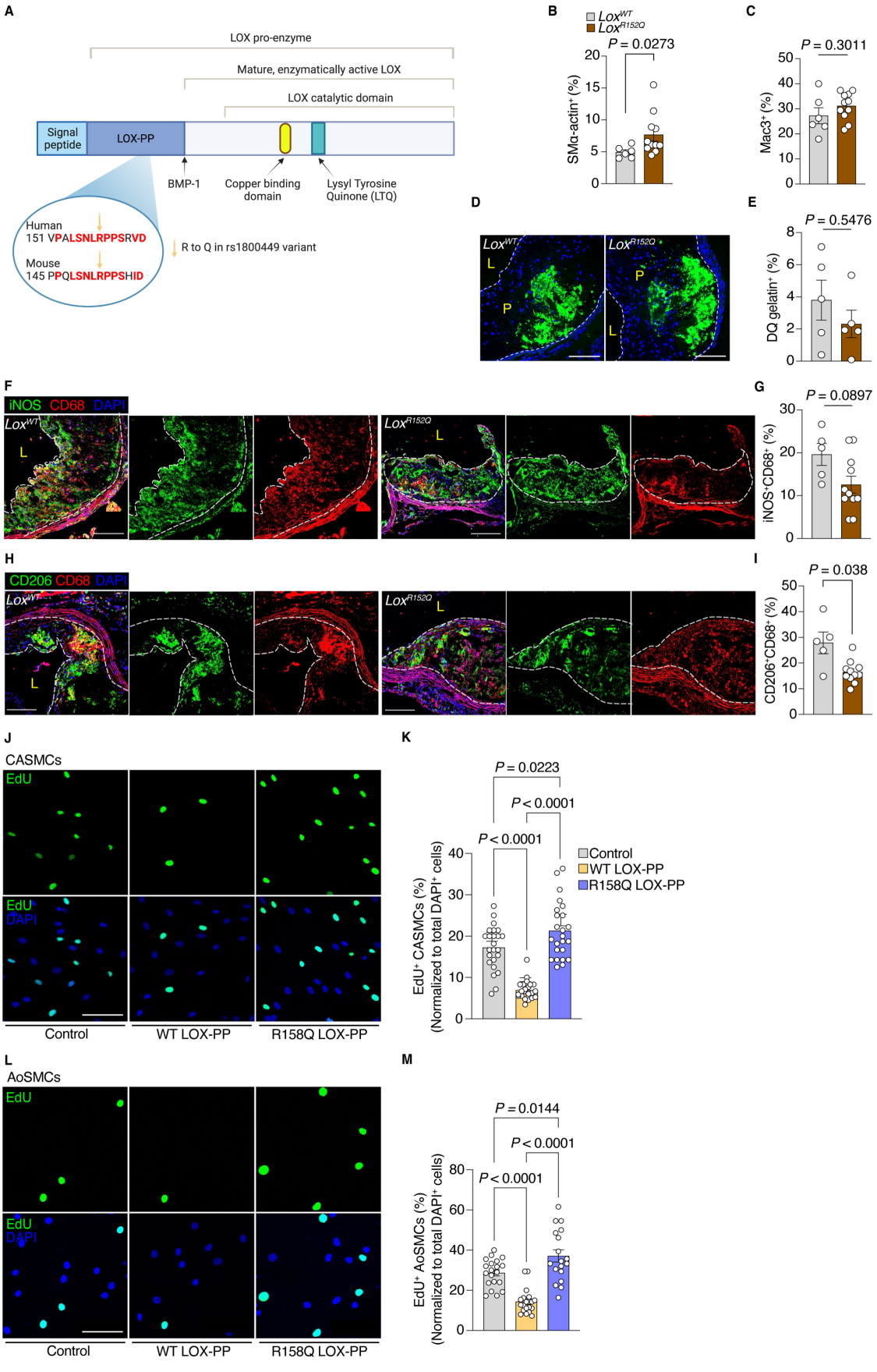
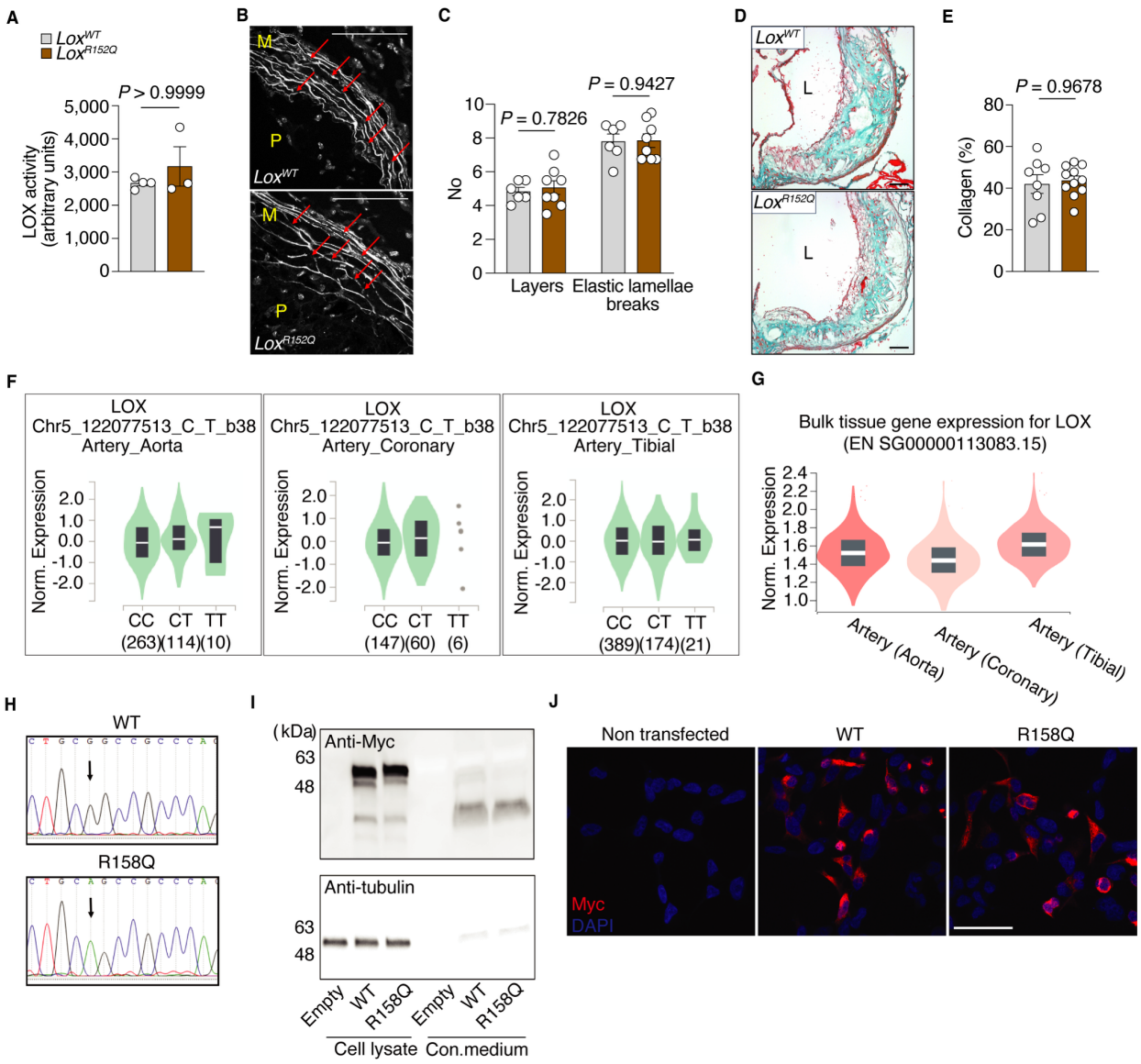
Supplementary Material

A loss of function polymorphism in the propeptide of lysyl oxidase exacerbates atherosclerosis

Figure	**Page**
Supplemental Figure 1.	2-3
Supplemental Figure 2.	4-5
Supplemental Figure 3.	6
Supplemental Figure 4.	7
Supplemental Figure 5.	8
Supplemental Figure 6.	9
Supplemental Table 1.	See attached spreadsheet
Supplemental Table 2.	See attached spreadsheet
Supplemental Table 3.	See attached spreadsheet

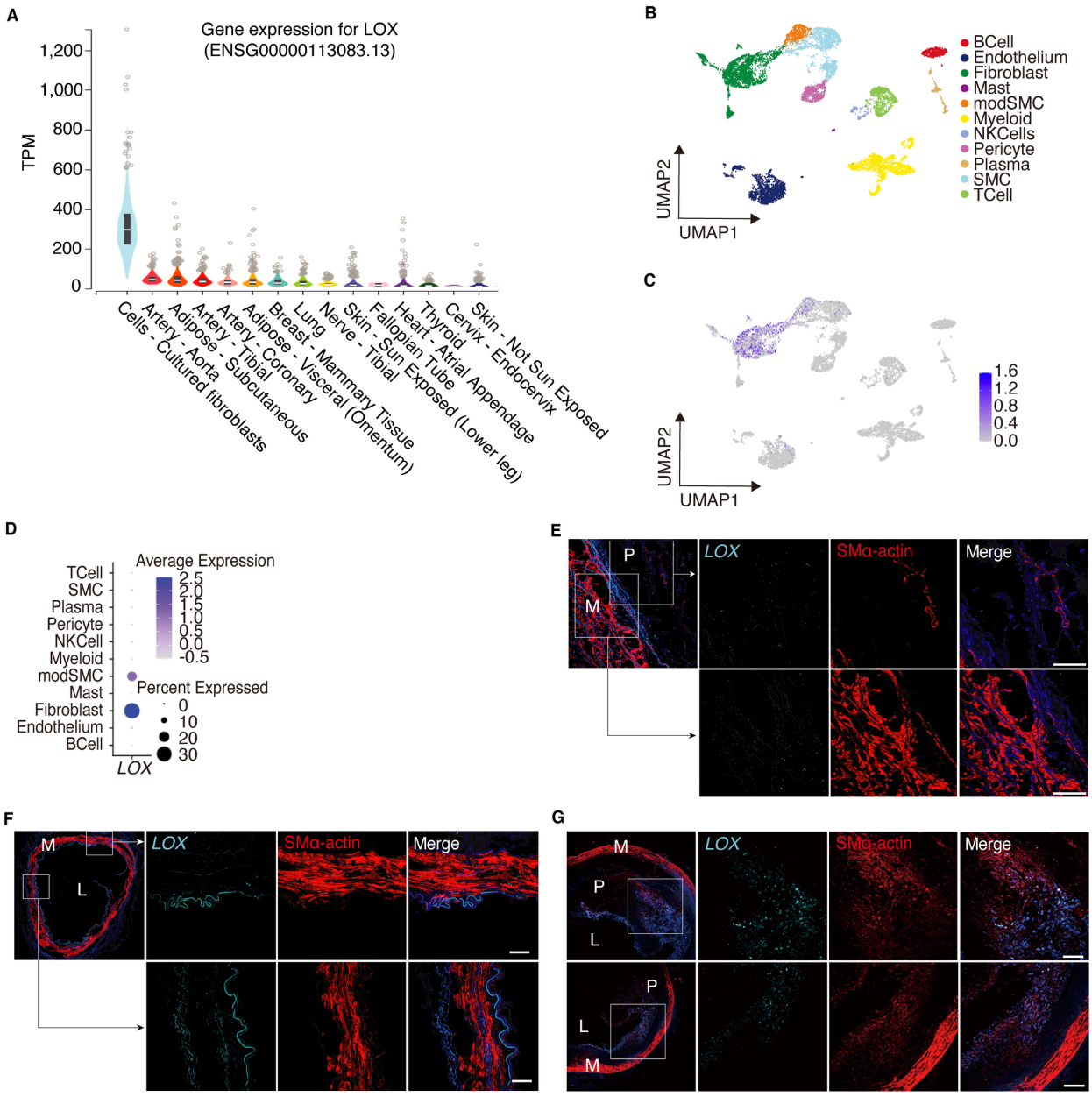

A
LOX pro-enzyme
Mature, enzymatically active LOX
LOX catalytic domain
Signal peptide
LOX-PP
BMP-1
Copper binding domain
Lysyl Tyrosine Quinone (LTQ)
Human
151 VPALSNLRPPSRVD
Mouse
145 PPQLSNLRPPSHID
R to Q in rs1800449 variant
B
LoxWT
LoxR152Q
P = 0.0273
SMα-actin+ (%)
C
P = 0.3011
Mac3+ (%)
D
LoxWT
LoxR152Q
L
P
E
P = 0.5476
DQ gelatin+ (%)
F
iNOS CD68 DAPI
LoxWT
LoxR152Q
L
G
P = 0.0897
iNOS+CD68+ (%)
H
CD206 CD68 DAPI
LoxWT
LoxR152Q
L
I
P = 0.038
CD206-CD68+ (%)
J
CASMCs
EdU
EdU
DAPI
Control
WT LOX-PP
R158Q LOX-PP
K
P = 0.0223
P < 0.0001
P < 0.0001
EdU+ CASMCs (%)
(Normalized to total DAPI+ cells)
Control
WT LOX-PP
R158Q LOX-PP
L
AoSMCs
EdU
EdU
DAPI
Control
WT LOX-PP
R158Q LOX-PP
M
P = 0.0144
P < 0.0001
P < 0.0001
EdU+ AoSMCs (%)
(Normalized to total DAPI+ cells)

Supplemental Figure 1. Atherosclerotic plaque complexity and in vitro proliferation assay of primary human vascular smooth muscle cells.
(A) Structural elements of the LOX. LOX is synthesized as pro-enzyme that is cleaved by the BMP-1 protease (by additional proteases such as ADAMTS2/14) to release the mature active enzyme. The catalytic domain is highly conserved among the different lysyl-oxidases and includes a conserved copper binding domain and a unique lysyl tyro sine quinone (LTQ) element that is essential for the catalytic activity. In the LOX-PP, conserved sequences around human residue R158 (mouse residue R152) were highlighted in red. Quantification of **(B)** SMα-actin and **(C)** Mac3 positive area as a percentage of plaque burden area as shown in Figure **1L** (n = 6-7/group). **(D)** Active MMP (DQ-gelatin) positive area by in situ zymography. **(E)** Quantification of DQ gelatin-stained area (green) as a percentage of plaque area (n = 5/group). **(F)** iNOS staining for inflammatory macrophage. **(G)** Quantification of $iNOS^+CD68^+$ double-positive-area as a percentage of plaque area (n = 5-11/group). **(H)** CD206 staining for reparative macrophage. **(I)** Quantification of $CD206^+CD68^+$ double-positive-area as a percentage of plaque area (n = 5-11/group). **(J** through **M)** Primary human coronary artery smooth muscle cells (CASMCs) and aortic smooth muscle cells (AoSMCs) were treated with vehicle control, 10 μg mL^{-1} wild-type (WT) LOX-PP, or R158Q LOX-PP for 48 hrs. Cells were then labeled with 10 μM of EdU (5-ethynyl-2'deoxyuridine) for 24 hrs and detected using an an Alexa Flour 488-containing reaction cocktail. **(J** and **L)** Representative images of EdU^+CASMCs and EdU^+AoSMCs under each treatment condition. **(K** and **M)** Quantification of EdU^+CASMCs and EdU^+AoSMCs as a percentage of total $DAPI^+$ cells. Control indicates cells treated with media alone. Scale bars, 100 μm. Data were analyzed with unpaired nonparametric Mann-Whitney test **(B, C, E, G, I)**, and one-way ANOVA followed by multiple-comparison testing **(K** and **M)** shown as the mean ± SEM. P, plaque; L, lumen.



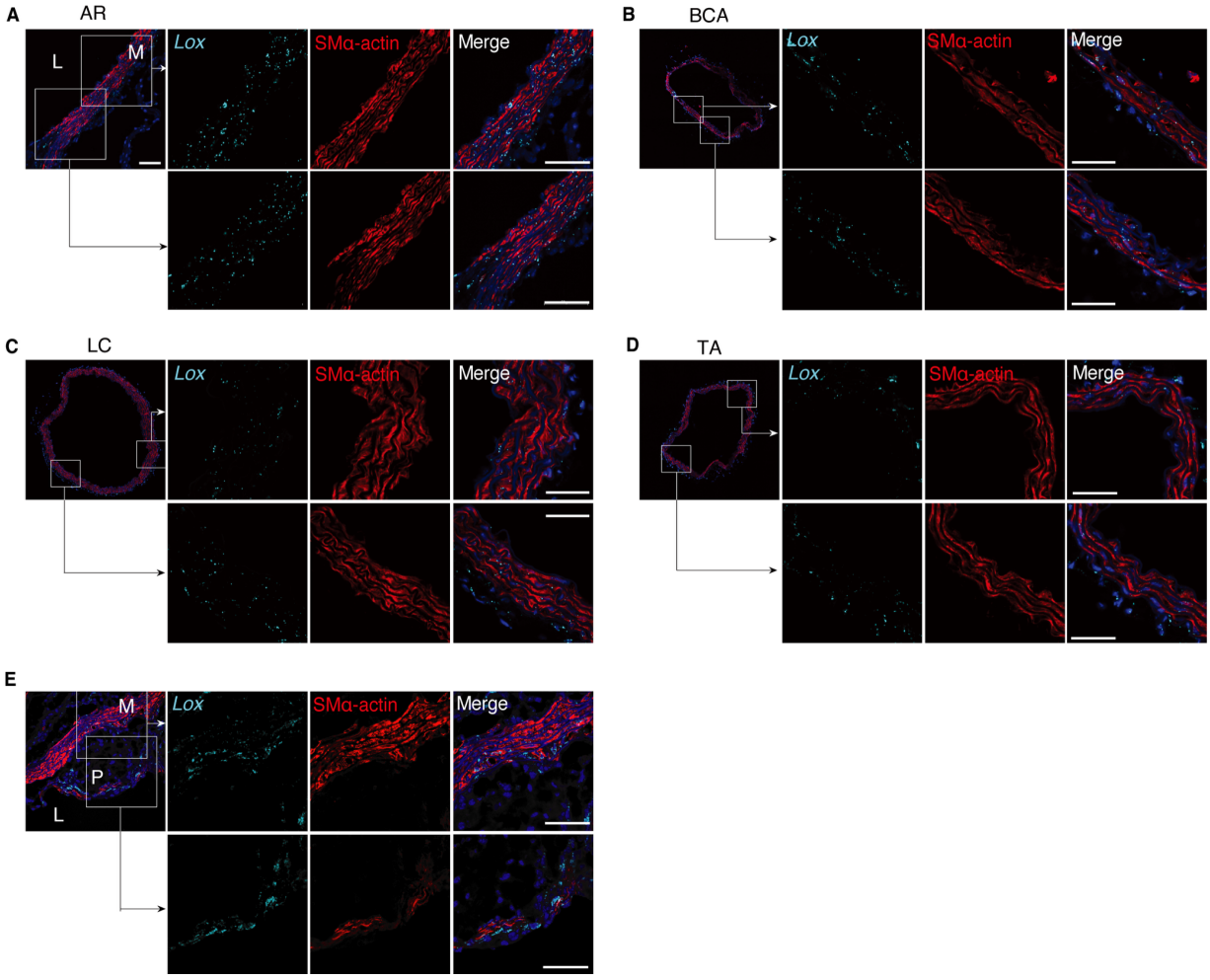
Supplemental Figure 2. The R158Q polymorphism is not associated with altered LOX enzyme activity, arterial matrix organization, or arterial LOX expression.
(A) LOX enzyme activity in aortic root tissues from Lox^{WT} ($n = 4$) and Lox^{R152Q} ($n = 3$) mice fed HFD for 16 weeks. The bars represent the activity in arbitrary units. **(B)** Representative images of autofluorescence of elastin in aortic root tissues. Red arrows indicate fragmented and disorganized elastic lamellae. **(C)** Number of layers and elastic lamellae breaks in aortic root from Lox^{WT} ($n = 6$) and Lox^{R152Q} ($n = 8$) mice fed HFD for 16 weeks. **(D)** Collagen staining by Masson's Goldner. **(E)** Quantification of collagen-stained area (green) as a percentage of plaque area (n = 8-11/group). **(F and G)** mRNA levels by genotype and arterial bed as measured in the GTEx project. There is no significant difference in *LOX* expression by genotype in aorta (P = 0.4), coronary artery ($P = 0.92$), and tibial artery ($P = 0.14$), and no difference in *LOX* expression by **(F)** arterial bed or **(G)** across arterial tissues. **(H)** Sequencing results to confirm the change in R158Q amino acid following site-directed mutagenesis. The successful G to A nucleotide change at position 473 is indicated by the arrows. *LOX WT* (upper), and *LOX R158Q* (lower). **(I)** Immunoblot of LOX proteins in HEK-293T cells. Cell lysate and concentrated conditioned

media from HEK-293T cells transfected with pCMV6 vector with non-transfected (empty), wild-type LOX, and R158Q LOX respectively were used and assessed by anti-Myc (upper panel). Anti-tubulin was used for protein loading control (lower panel). **(J)** Cells were stained with anti-Myc (red) to visualize LOX expression. DAPI for nuclei was shown in blue. Scale bars, 100 μm **(B** and **D)**, 50 μm **(J)**. Data were analyzed with unpaired nonparametric Mann-Whitney test, and shown as the mean ± SEM. P, plaque; L, lumen; M, media.

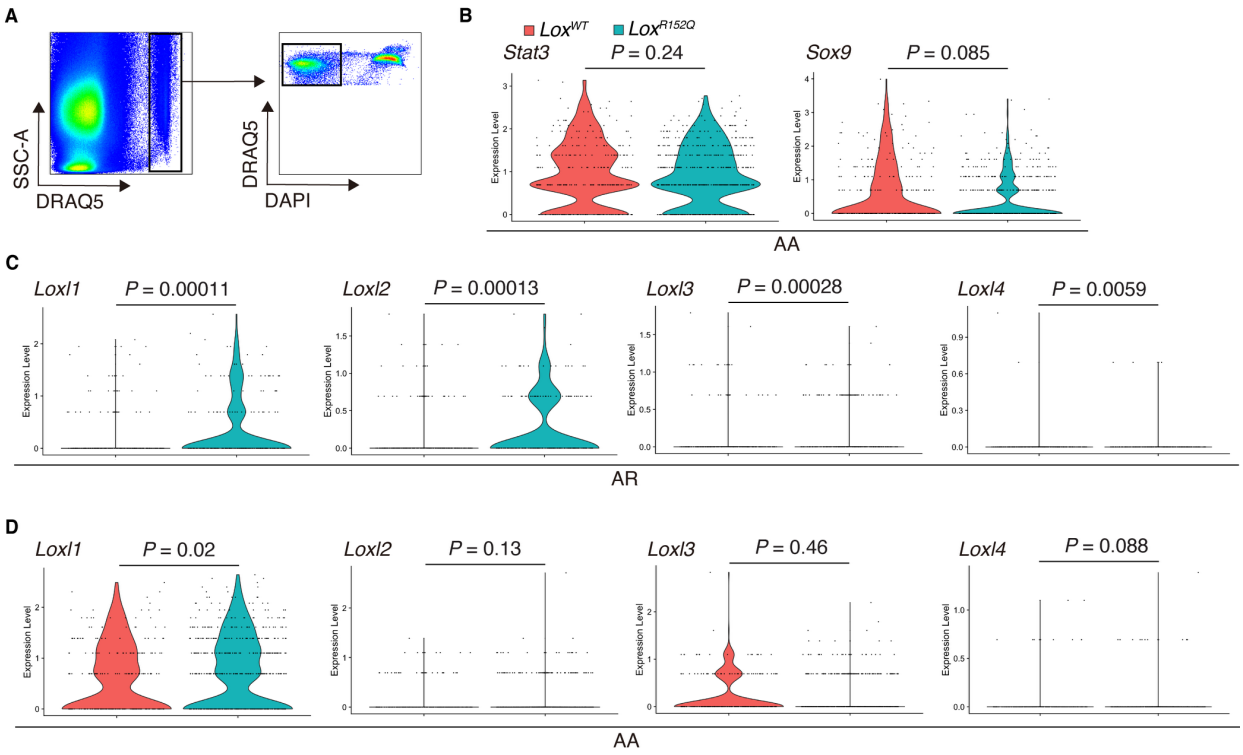


Supplemental Figure 3. *LOX* expression by VSMCs in arteries under atherosclerotic conditions in human.

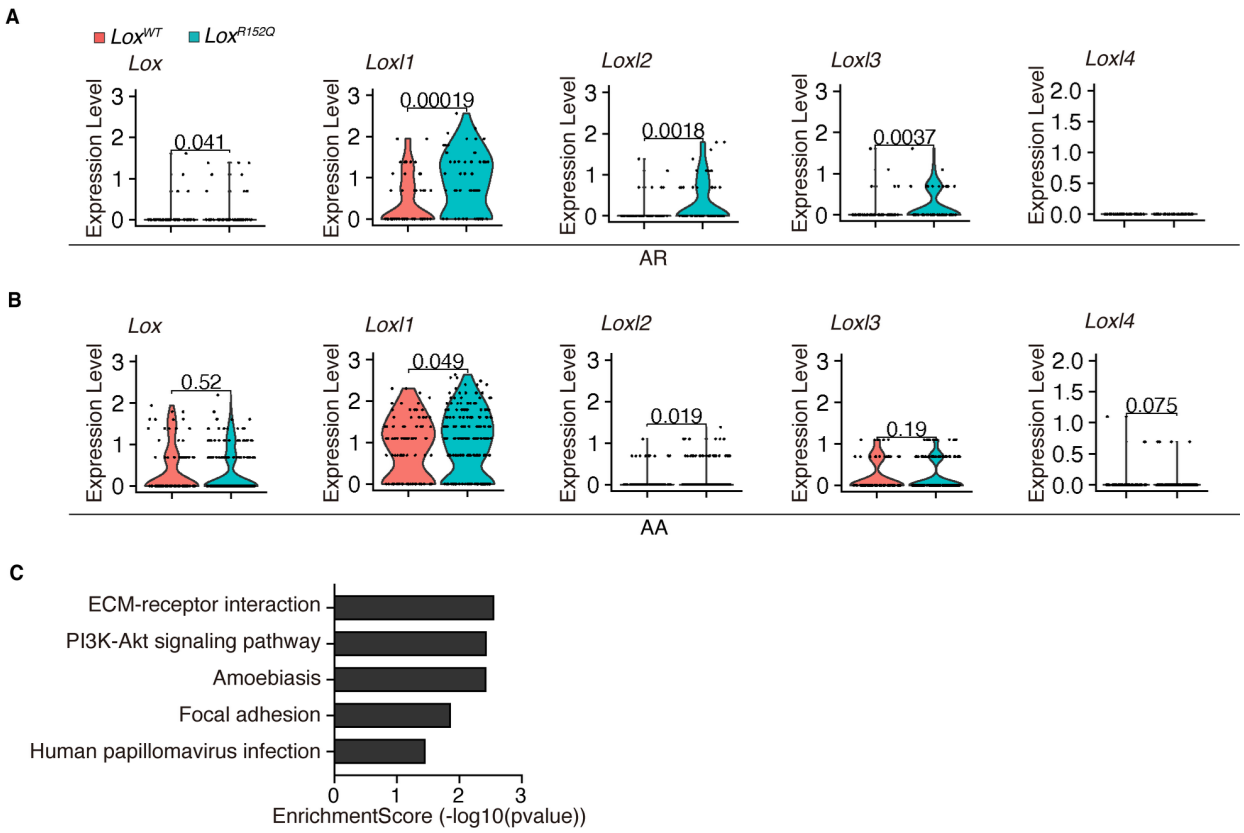
(A) List of GTEx tissues in order of *LOX* expression levels. **(B)** Uniform Manifold Approximation and Projection (UMAP) embedding plot with cell types present in the human coronary artery. **(C)** Expression of *LOX* on the UMAP. **(D)** Dot plot of *LOX* for cell types. **(E** through **G)** Expression of *LOX* in **(E)** human aortic wall, **(F)** LIMA, and **(G)** coronary artery frozen cross sections from patients using RNAscope ISH. Outlined areas indicate the regions magnified in the next panels. Tissues were co-stained with the VSMC marker, SMα-actin. Scale bars, 50 μm. P, plaque; M, media; L, lumen.



Supplemental Figure 4. *Lox* expression by VSMCs in mouse arteries.
Expression of *Lox* using RNAscope ISH in the **(A)** aortic root, **(B)** BCA, **(C)** LC, and **(D)** TA from 8-week-old chow diet-fed *Apoe*$^{-/-}$ mice. **(E)** Expression of *Lox* in the aortic root from 8 weeks of HFD-fed *Apoe*$^{-/-}$ mice. Outlined areas indicate the regions magnified in the next panels. All tissues were co-stained with the VSMC marker, SMα-actin. Scale Bars, 50 μm. P, plaque; M, media; L, lumen.



Supplemental Figure 5. Comparison of expression levels of *Lox* family members in mouse aortic vessels.
(A) Flow cytometry cell sorting strategies. DRAQ5-positive and DAPI-negative ($DRAQ5^{+}DAPI^{-}$) cells were subjected to single-cell RNA sequencing. **(B)** Comparison of *Stat3, Sox9* expression in the ascending aorta between genotypes. **(C** and **D)** Expression levels of *Lox* family members (*Loxl1* through *Loxl4*) in aortic root **(C)**, and ascending aorta **(D)**.



Supplemental Figure 6. Expression of *Lox* family members and signaling pathways in fibroblasts.
(A and **B)** Expression levels of *Lox* family members (*Lox*, *Loxl1* through *Loxl4*) in fibroblasts from the aortic root **(A)**, and ascending aorta **(B)**. **(C)** Pathway analysis on differential analysis. Top 5 pathways enriched in the aortic root fibroblasts from Lox^{R152Q} mice compared to controls.